Crystallization of hepatitis B virus core protein shells: determination of cryoprotectant conditions and preliminary X-ray characterization

**S. A. Wynne, A. G. W. Leslie,*
P. J. G. Butler and R. A.
Crowther**

MRC Laboratory of Molecular Biology, Hills
Road, Cambridge CB2 2QH, England

Correspondence e-mail:
andrew@lmb-mrc.cam.ac.uk

Hepatitis B virus causes liver cirrhosis and hepatocellular cancer and is a major cause of death, particularly in Asia and sub-Saharan Africa. The virus consists of an inner core or nucleocapsid, which encloses the viral nucleic acid, with an outer lipid envelope containing surface-antigen proteins. The core protein, when expressed in *E. coli*, assembles into spherical shells containing 180 or 240 subunits, arranged with $T = 3$ or $T = 4$ icosahedral symmetry. The C-terminal region of the protein is involved in nucleic acid binding, and deletion of this region does not prevent capsid formation. C-terminally deleted hepatitis B core shells containing 240 subunits have been crystallized and data has been collected to 3.6 Å resolution from frozen crystals, using butanediol as a cryoprotectant. The crystals have $C2$ symmetry, with unit-cell parameters $a = 538.0$, $b = 353.0$, $c = 369.6$ Å, $\beta = 132.3°$.

1. Introduction

Hepatitis B virus is a member of the hepadnavirus family. It causes worldwide health problems, as chronic infection can result in viral hepatitis, cirrhosis and cancer of the liver. The virus consists of a lipid envelope containing surface-antigen proteins, surrounding an inner nucleocapsid or core which packages the viral DNA. The capsid is composed of identical subunits encoded by a single viral gene which, when expressed in *Escherichia coli*, produces two sizes of icosahedral shell made up of 180 subunits ($T = 3$) or 240 subunits ($T = 4$), with overall diameters of 320 and 360 Å, respectively. The local packing in both sizes of capsid is similar, with dimers of subunits forming protruding spikes (Crowther *et al.*, 1994). The C-terminal region of the core subunit is very basic and is believed to interact with the viral nucleic acid (Birnbaum & Nassal, 1990). This region is not believed to be directly involved in capsid formation because core subunits with the basic C-terminal region deleted still assemble into shells (Gallina *et al.*, 1989). However, truncation does affect the ratio of $T = 4$ to $T = 3$ particles, with longer deletions increasing the proportion of $T = 3$ capsids (Zlotnick *et al.*, 1996).

The hepatitis B core shell is being studied in order to solve the structure of the core protein and to determine the interactions between the core-protein subunits involved in capsid formation. Recently, a three-dimensional map of the $T = 4$ hepatitis B core shell was determined by electron cryomicroscopy at 7.4 Å resolution, which revealed the protein fold (Böttcher *et al.*, 1997). This map will be used to provide phase information for X-ray diffraction data. Here we describe crystallization and preliminary crystallographic characterization of the $T = 4$ capsids, including the determination of the particle orientation in the unit cell.

2. Materials and methods

2.1. Cloning of the hepatitis core proteins

Core proteins from four different strains of hepatitis B were truncated at residue 149: a Latvian isolate of hepatitis B (HBc-Riga; Bichko *et al.*, 1985), a strain of hepatitis B isolated at St Mary's Hospital in London (HBc-CW), a hepatitis B strain obtained from Professor K. Murray in Edinburgh (HBc-Edin; Pasek *et al.*, 1979) and a woodchuck hepatitis strain (WHV). There are six differences in amino-acid sequence between HBc-Riga and HBc-CW, eight between HBc-Riga and HBc-Edin and 54 differences between HBc-Riga and the WHV core protein.

PCR primers were designed to introduce an *Nde*I site at the ATG initiation codon and a stop codon plus *Eco*RI site after residue 149. The PCR products were cleaved with *Nde*I and *Eco*RI and ligated into the vector PT7-SC (US Biochemicals). These C-terminally deleted constructs were named HBcΔ-Riga, HBcΔ-CW, HBcΔ-Edin and WHVΔ.

2.2. Purification of the core proteins

BL21 (DE3) cells were transformed with the relevant plasmids and cultures were grown in 2× YT broth to an OD_{600} of 0.7–1.0. The cultures were induced with isopropyl-β-D-thiogalactopyranoside (IPTG) to a final

crystallization papers

concentration of 4 µM and grown for a further 3 h before harvesting. Cells were lysed by freeze-thawing three times in lysis buffer [50 mM Tris–HCl pH 8.0, 5 mM EDTA, 100 µg ml⁻¹ phenylmethylsulfonyl fluoride (PMSF), 2 mg ml⁻¹ lysozyme], using 20 ml lysis buffer per litre of cell culture. Following lysis, 0.1 M MgCl$_2$ and 0.2 mg ml⁻¹ DNAase were added (2 ml per litre of cell culture) and the mixture was incubated at room temperature for 10 min before centrifugation at 15 000 rev min⁻¹ for 30 min to remove cell debris.

(a)

(b)

(c)

400 µm

Figure 1
Hepatitis B core-protein (HBc-Riga) crystals grown in decreasing concentrations of (NH$_4$)$_2$SO$_4$, showing the improvement in crystal morphology: (a) 0.5 M, (b) 0.3 M, (c) 0.2 M.

(NH$_4$)$_2$SO$_4$ was added to the supernatant to 50% for the preparation of C-terminally deleted forms of the Riga, Edinburgh and WHV strains, and to 30% for the preparation of HBcΔ-CW. The precipitate was pelleted at 15 000 rev min⁻¹. The pellet was resuspended in Tris-buffered saline (TBS) containing 0.1% Triton X-100 and passed down a Sepharose CL-4B column. Fractions containing the core protein were detected by SDS–PAGE, pooled and precipitated with 50% (NH$_4$)$_2$SO$_4$. When examined by electron microscopy, the preparations comprised approximately 98% $T = 4$ shells and 2% $T = 3$ shells. The precipitate was resuspended in TBS, dialysed against TBS for 4 h and layered onto 10–40% sucrose gradients in a SW28Ti rotor. Centrifugation for 17 h at 28 000 rev min⁻¹ allowed the separation of $T = 4$ from $T = 3$ core shells. Fractions from the leading edge of the peak were pooled, dialysed against 5 mM Tris–HCl, 150 mM NaCl and finally concentrated in a Sartorius concentration unit to 40 mg ml⁻¹ core protein. The quality and purity of preparations were routinely checked by electron microscopy.

2.3. Crystal growth

Crystallization conditions were screened by the hanging-drop (vapour-diffusion) method using Linbro multiwell tissue-culture plates. The drops were set up with 2 µl of core protein and 2 µl of well buffer. The Hampton crystal screens I and II (Hampton Research) were used to determine initial precipitation conditions for each of the four core proteins. A range of protein concentrations between 5 and 25 mg ml⁻¹ was used and crystallization trials were set up at several temperatures between 280 and 299 K. Conditions that gave crystalline precipitates in the hanging drops were identified and optimized further. D(−)-2,3-butanediol used in cryoprotectant trials was obtained from Fluka.

2.4. X-ray analysis

Diffraction experiments at room temperature were carried out with crystals mounted in standard glass capillary tubes. When cryocooling, crystals were soaked in the appropriate cryoprotectant in glass depression wells and then frozen directly in the 100 K N$_2$ gas stream from an Oxford Cryosytems Cryostream. X-ray analysis was carried out in the laboratory using an Elliot GX21 rotating-anode generator equipped with double-mirror (Supper) collimation and a 30 cm MAR Research image-plate scanner. Synchrotron X-ray data were collected at station ID2 at ESRF, Grenoble, and station 9.6 at the SRS, Daresbury, in both cases using a 30 cm MAR Research image-plate detector. Diffraction data were integrated with *MOSFLM* (Leslie, 1992) and processed with programs from the *CCP*4 suite (Collaborative Computational Project, Number 4, 1994). Self-rotation functions were calculated with the program *GLRF* (Tong & Rossmann, 1997).

3. Results and discussion

3.1. Crystallization

A number of conditions from the Hampton screens gave crystals of core protein, and these conditions were refined to give sharp faceted crystals.

Crystallization conditions using various concentrations of PEG 20000 and (NH$_4$)$_2$SO$_4$ gave clusters of crystals of HBcΔ-Riga and HBcΔ-CW that resembled balls of string. The nucleation was very sensitive to the exact precipitant concentration, and small reductions in the (NH$_4$)$_2$SO$_4$ concentration finally yielded single crystals from the large clusters, as illustrated in Fig. 1.

The best crystals were produced from the HBcΔ-CW protein using 3.5–4.5% PEG 20000 and 0.45–0.55 M (NH$_4$)$_2$SO$_4$ as precipitants and 0.1 M 2-(N-morpholino) ethanesulfonic acid (MES) pH 6–7 as a buffer. These conditions yielded large faceted plate-like crystals between 0.4 and 1.5 mm long and between 0.02 and 0.15 mm thick (Fig. 2a) over a period of two weeks to six months. The best of these crystals diffracted to 4.6 Å in the laboratory. Addition of 0.4% β-octylglucoside improved the thickness of the crystal plates, but the diffraction limit remained at best 4.6 Å. In spite of the small number of differences in amino-acid sequence, the three other core-protein shells produced poorer quality crystals, with HBcΔ-Riga crystals diffracting to 23 Å and the crystals of HBcΔ-Edin and WHVΔ failing to produce any diffraction.

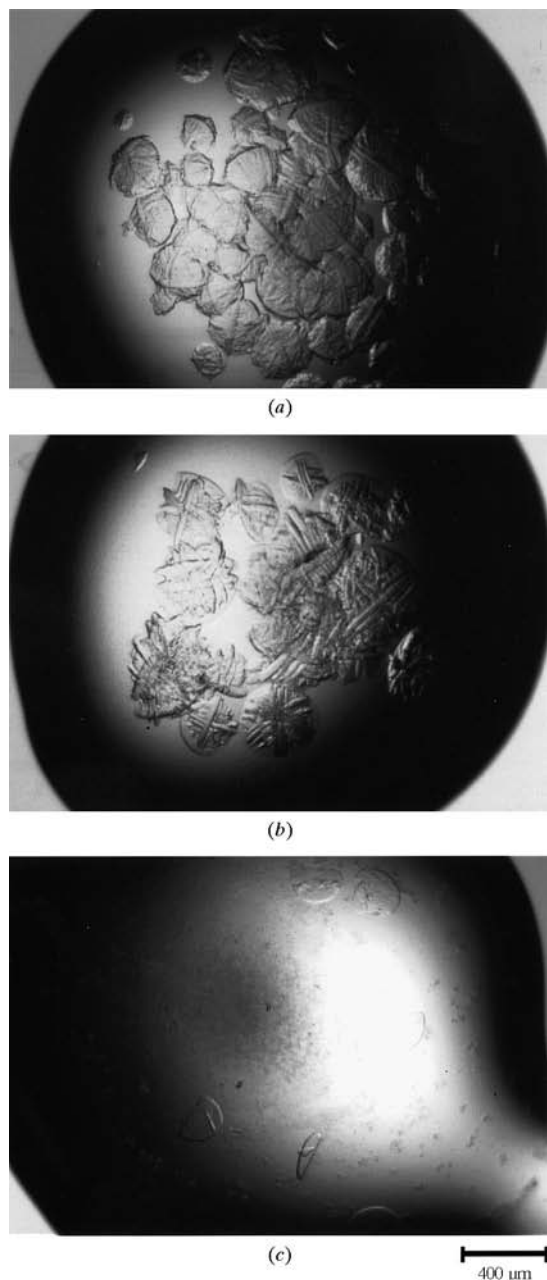The temperature was varied between 280 and 299 K to optimize crystal formation. The

best crystals formed from the 4% PEG screen at 292 K. A range of protein concentrations (between 10 and 25 mg ml^{-1}) was also used, and found to influence the rate of crystal growth, with 15 mg ml^{-1} HepBcΔ-CW giving the most reproducible crystals. Seeding was attempted to reduce the occurrence of twinning and clustering but was not successful under any conditions.

3.2. Room-temperature diffraction experiments

The plate-like crystals from the 4% PEG screen diffracted well to 4.6 Å in the laboratory or 3.5 Å at the SRS, but were very sensitive to radiation, and it was only possible to collect two or three images from each crystal. There was also considerable crystal slippage within the capillary, preventing useful data collection. Conditions for cryocooling the crystals were therefore investigated in an attempt to circumvent both these difficulties.

3.3. Cryoprotectants

Glycerol, MPD (2-methyl-2,4-pentanediol), ethylene glycol, PEG 400, sucrose, glucose, xylitol, *meso*-erythritol and D(−)-

(a)

(b)

200 μm

Figure 2
(*a*) A crystal of HBcΔ-CW grown in 4% PEG 20 000, 0.5 M (NH$_4$)$_2$SO$_4$ and 0.1 M MES pH 6.5. (*b*) A crystal of HBcΔ-CW grown in 4% PEG 20 000, 0.5 M (NH$_4$)$_2$SO$_4$, 0.1 M MES pH 6.5 and 15% butanediol.

2,3-butanediol (butanediol) have all previously been used successfully as cryoprotectants (Rodgers, 1994). These compounds were added to the crystallization buffer [0.1 M MES pH 6.5, 0.5 M (NH$_4$)$_2$SO$_4$, 4% PEG, 1 mM MgCl$_2$] at concentrations between 5 and 40%, and crystals from the 4% PEG screen were swiped through these solutions and frozen in the N$_2$ gas stream. Even when using the highest concentrations of cryoprotectant, the crystals were opaque when frozen and did not diffract. As an alternative approach, crystals were soaked in increasing concentrations of the cryoprotectant solutions (using 5% steps) for varying lengths of time between 30 s and 30 min per step. The crystals were then frozen in the N$_2$ gas stream.

The X-ray diffraction images showed that the best cryoprotectant for soaking was ethylene glycol, and in this case diffraction was observed to 5 Å in the laboratory.

3.4. Growth of crystals in cryoprotectant

Further crystal screens were set up with HBcΔ-CW, incorporating different concentrations of cryoprotectants with varying concentrations of (NH$_4$)$_2$SO$_4$ and PEG 20 000. Many of the cryoprotectants inhibited the growth of crystals completely, but crystals did form in the presence of MPD, glycerol and butanediol. These crystals were frozen in the N$_2$ gas stream at 100 K and their diffraction was measured. The results in Table 1 show that crystals grown in the presence of 12 or 15% butanediol, when soaked for 5 min in crystallization buffer containing 20% butanediol immediately prior to freezing, gave good diffraction to 6 Å in the laboratory.

The best crystals grew in 0.1 M MES pH 6.5, 0.5 M (NH$_4$)$_2$SO$_4$, 4% PEG 20 000 and 12% butanediol at protein concentrations between 15 and 25 mg ml^{-1}. These were triangular plates with typical dimensions of 0.4 × 0.4 × 0.05 mm (Fig. 2*b*).

3.5. Crystallographic characterization

Crystals grown in 12–15% butanediol and then soaked in 20% butanediol immediately prior to freezing were used to collect a 3.6 Å resolution data set on station ID2 at the ESRF, Grenoble. The space group was determined to be C2, with unit-cell parameters a = 538.0, b = 353.0, c = 369.6 Å, β = 132.3°. Data from four crystals were merged to give a data set that was 96%
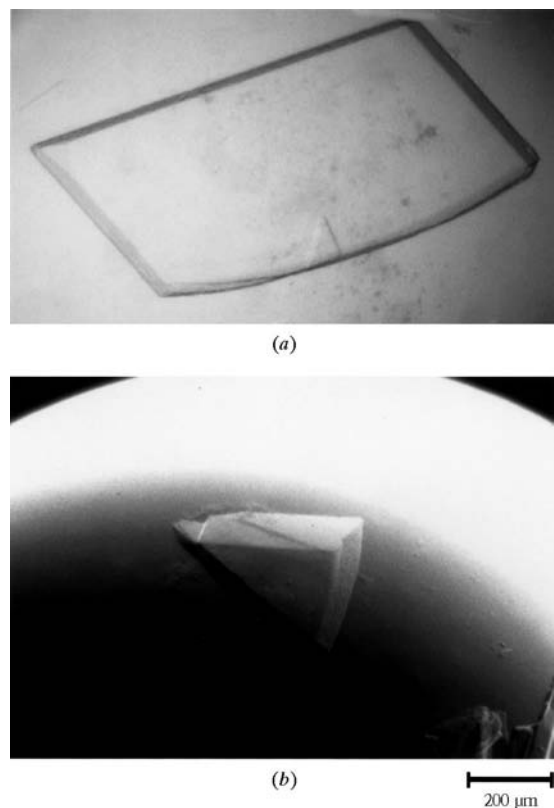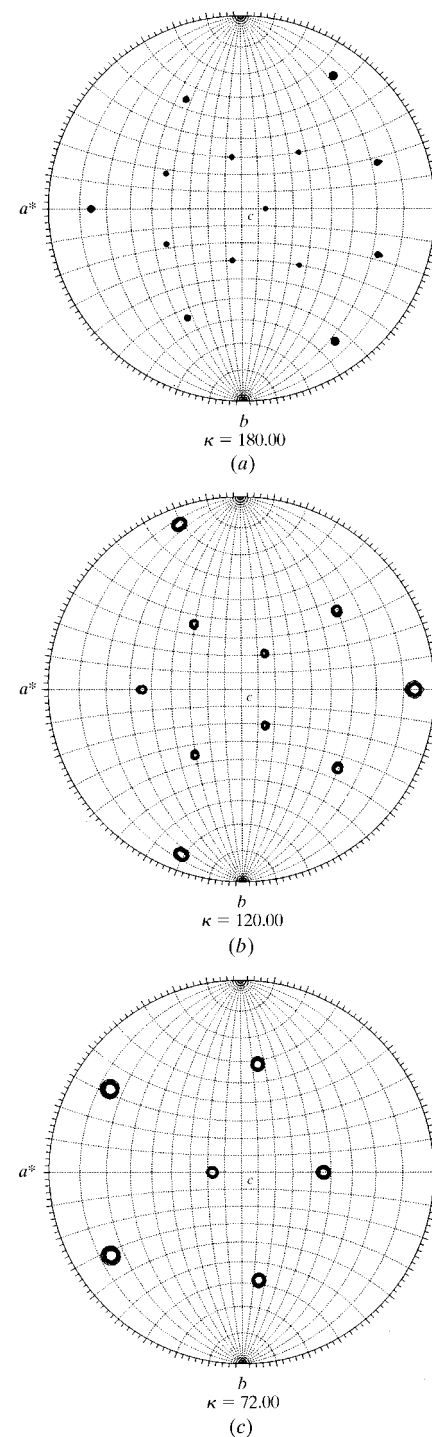

(a)

(b)

(c)

Figure 3
Stereographic projections of the self-rotation functions calculated using data between 5 and 20 Å resolution and an integration radius of 140 Å. All the expected icosahedral symmetry axes are present at levels well above noise. (*a*) κ = 180° section, (*b*) κ = 120° section, (*c*) κ = 72° section.

crystallization papers

Table 1
Growth of HBcΔ-CW crystals in the presence of cryoprotectants.

The cryoprotectants were added to 0.1 *M* MES pH 6.5, 1 m*M* MgCl$_2$ and a range of concentrations of PEG 20 000 (3–5%) and (NH$_4$)$_2$SO$_4$ (0.05–0.5 *M*). Crystals were grown in hanging drops and their diffraction measured on a laboratory source at 100 K.

Cryoprotectant	Crystal formation	Diffraction limit (Å)
Glycerol	Well faceted crystals grew in 15% glycerol	No diffraction
MPD	Well faceted crystals grew in 25% MPD	7.5
MPD with glycerol	Large faceted crystals grew in 25% MPD, 1% glycerol	7.5
Butanediol	Well faceted crystals grew in 12 and 15% butanediol. Crystals were soaked in 20% butanediol for 5 min prior to freezing	6

complete to 3.6 Å resolution, with a merging *R* factor (on intensities) of 16%. In the outer resolution shell (3.8–3.6 Å) the completeness was 95% and the merging *R* factor was 60%. The crystal mosaic spread varied between 0.4 and 0.6° for different crystals, but the cell dimensions were identical within experimental error. Although it is probable that freezing was responsible for the relatively high mosaic spread (more typically 0.1–0.2° for virus crystals), this has not been verified as no data were collected from unfrozen crystals grown in the presence of butanediol.

Packing considerations suggested that an icosahedral twofold axis of the particle was coincident with the crystallographic twofold axis. Self-rotation functions calculated using data between 5 and 20 Å resolution with an integration radius of 140 Å confirmed this (Fig. 3) and also displayed all the expected icosahedral symmetry axes. The $\kappa = 180°$ section of the self-rotation function also shows that an icosahedral twofold axis lies 14.5° away from the *c* axis, which uniquely defines the particle orientation in the unit cell. The position of the particle along the *b* axis is arbitrary in this space group. The 7.4 Å resolution model derived by electron cryomicroscopy (Böttcher *et al.*, 1997) can now be placed in the crystallographic unit cell to provide an initial phasing model. The 30-fold non-crystallographic symmetry will be used to extend the phases to 3.6 Å resolution.

References

Bichko, V., Pushko, P., Dreilina, D., Pumpens, P. & Gren, E. (1985). *FEBS Lett.* **185**, 208–212.

Birnbaum, F. & Nassal, M. (1990). *J. Virol.* **64**, 3319–3330.

Böttcher, B., Wynne, S. A. & Crowther, R. A (1997). *Nature (London)*, **386**, 88–91.

Collaborative Computational Project, Number 4 (1994). *Acta Cryst.* D**50**, 760–763.

Crowther, R. A., Kiselev, N. A., Böttcher, B., Berriman, J. A., Borisova, G. P., Ose, V. & Pumpens, P. (1994). *Cell*, **77**, 943–950.

Gallina, A., Bonelli, F., Zentilin, L., Rindi, G., Muttini, M. & Milanesi, G. (1989). *J. Virol.* **63**, 4645–4652.

Leslie, A. G. W. (1992). *Jnt CCP4 EST-EACMB Newsl. Protein Crystallogr.* **26**.

Pasek, M., Goto, T., Gilbert, W., Zink, B., Schaller, H., MacKay, P., Leadbetter, G. & Murray, K. (1979). *Nature (London)*, **282**, 575–579.

Rodgers, D. W. (1994). *Structure*, **2**, 1135–1140.

Tong, L. & Rossmann, M. G. (1997). *Methods Enzymol.* **276**, 594–611.

Zlotnick, A., Cheng, N., Conway, J. F., Booy, F. P., Steven, A. C., Stahl, S. J. & Wingfield, P. T. (1996). *Biochemistry*, **35**, 7412–7421.